Taylor & Francis
Taylor & Francis Group

Enhancing Dielectric Properties of Poly(vinylidene fluoride)-Based Hybrid Nanocomposites by Synergic Employment of Hydroxylated BaTiO$_3$ and Silanized Graphene

Mei Du[b], Wei Wang[a], Lei Chen[a], Zhiwei Xu[a], Hongjun Fu[a], and Meijun Ma[a]

[a]Key Laboratory of Advanced Braided Composites, Ministry of Education, School of Textiles, Tianjin Polytechnic University, Tianjin, People's Republic of China; [b]Textile and Garment Institute, Yancheng Institute of Industry Technology, Yancheng, People's Republic of China

ABSTRACT

The poly(vinylidene fluoride)-based hybrid composites with a blended BaTiO$_3$–exfoliated graphene as filler were fabricated with the efficient method of solution casting and hot pressing and their dielectric properties were investigated in detail. In advance, both of the nanoparticles are functionalized to improve the interfacial bonding between fillers and matrix. Synergistic effects arising from blending zero-dimensional BaTiO$_3$ and two-dimensional exfoliated grapheneare identified by the improved distribution of nanoparticles in poly(vinylidene fluoride) host and mitigating the concomitant increase in dielectric loss while maintaining the high dielectric constant values of the composites.

GRAPHICAL ABSTRACT
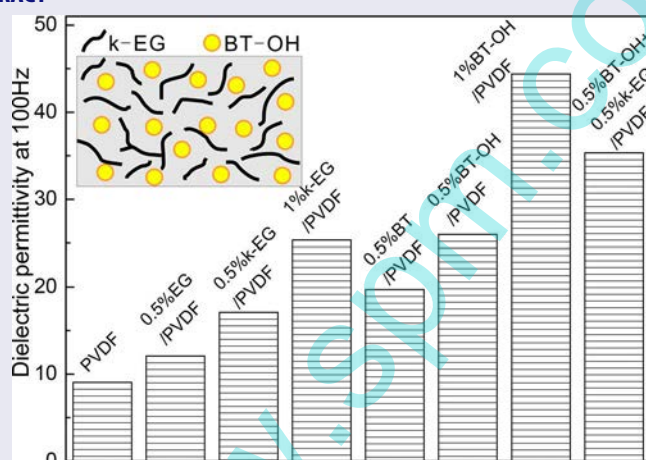
Introduction

Poly(vinylidene fluoride) (PVDF) copolymers are considered ideal candidates for several applications including electroacoustic and electromechanical convertors, actuators, ferroelectric memory devices, mechatronics, and artificial muscles for its fascinating piezoelectricity and improved mechanical behavior[1–13]. PVDF ceramic nanocomposites are currently of considerable interest as solution processable high-permittivity materials[14–23]. These nanocomposites can have both high permittivity and high dielectric strength. However, the high surface energy of dielectric nanoparticles usually leads to agglomeration and phase separation from the PVDF, resulting in poor processability of the films and a high defect density[24]. In addition, the poor filler/matrix nanoscale interfacial adhesion also causes difficulties in suppressing the dielectric loss of the composites[10,15,19,25–28]. A great deal of work has been done on functionalizing nanoparticles with various methods to endow the composites with high performance including high dielectric constant and good thermal stability[4,29–34]. Nevertheless, in some case,

---

high dielectric constant inevitably associated with high dielectric loss[35], which may be caused by the leakage current among conductive fillers[36,37].

Lots of previous studies demonstrated that conductive materials coatings on the ceramic particles could result in enhanced dielectric performances in the polymer-based composites[38–44]. Luo et al. had reported that the nanosized Ag particles discretely deposited on the BaTiO$_3$ (BT) surface can efficiently enhance the dielectric permittivity of the composite. Theoretical calculations suggested that the enhanced permittivity of BT–Ag/PVDF composites should arise from the ultrahigh permittivity of BT–Ag fillers, which was over 10^4[45]. Liu et al.[46] reported the preparation of carbon nanotubes adhering BT nanoparticles through chemical vapor deposition. With an increase in nanoparticle content, the dielectric constant of composites remarkably increased, but the loss tangent gradually decreased, the dielectric constant of the composites was increased to 27.7 at 50 Hz. Zhang et al. fabricated a novel hybrid BT–graphene nanoplatelets by a sol–gel process at 800°C and then prepared PVDF-based composites with the hybrid nanoparticles[35]. The aggregation of graphene was thought to be inhibited and a linkage between graphene and BT was formed. Generally, it was found that all of these studies can lead to significant improvements in dielectric properties. However, the preparation process of the hybrid fillers is complex and the efficiency is suspected to be limited.

In this paper, we report a PVDF composite reinforced by the blended fillers of BT and exfoliated graphene (EG). The thought is to integrate the advantages of the different dimensional materials to mitigate the concomitant increase in dielectric loss while maintaining the high dielectric constant values. The strategy for preparing the hybrid nanocomposites is the efficient solution casting and hot pressing method. Before fabricating composites, both of the nanoparticles are first functionalized by hydrogen peroxide (H$_2$O$_2$) and (3-aminopropyl)triethoxysilane (APTES, a silane coupling agent) to get the BT-OH and silane-treated EG, respectively. Second, the functionalized nanoparticles are characterized by Fourier transform infrared spectroscopy (FTIR) and atomic force microscopic (AFM). The freeze-fractured cross sections of nanocomposite films are investigated using a scanning electron microscope (SEM). Energy dispersive spectrometer is used to characterize the dispersion of the fillers in composites. At last, the dielectric performances of the composites are tested. For comparison, the composites reinforced by EG, BT, k-EG, and BT-OH with various filler contents are also prepared and characterized.

Experimental

Materials

BaTiO$_3$ nanoparticles, average size of 40 nm, were purchased from Zhenjiang Airick Electronic material Co., Ltd, China. Natural graphite powder was provided by Nanjing Xianfeng Nanomaterial Science and Technology Co., Ltd, China. PVDF (FR904) was purchased from Shanghai 3 F New Materials Co., Ltd, China. N,N-dimethylacetamide (DMAc, >99.5%, reagent) was purchased from Tianjin Weichen Chemical Reagent Co., Ltd, China. APTES with purity of 95% (supplied by Tianjin Chemical Reagent No.1 Plant) was used as the silane functionalization agent. Other reagents were purchased from Tianjin Reagents Co., Ltd and used without further purification.

Preparation of EG

Exfoliated graphene was prepared by a two-step synthesis. First, graphite oxide was prepared by the modified Hummers method and then EG was obtained by thermal exfoliation from graphite oxide. In detail, a 9:1 mixture of concentrated H$_2$SO$_4$ and H$_3$PO$_4$ was added to a mixture of natural graphite flakes and KMnO$_4$, and the reaction was heated to 50°C and stirred for 12 h. The reaction was cooled to room temperature and poured into ice (400 mL) with H$_2$O$_2$ (30%, 3 mL). Then, the mixture was washed with deionized water until the pH value was up to 6, and then vacuum-dried at 60°C for 48 h. Finally, the prepared graphite oxide was thermally exfoliated in a vacuum tube furnace at the temperature of 1,050°C for 30 s, yielding the EG.

Silanization of EG

A total of 3.5 mL of 1.75 wt% APTES was added into a mixture (250 mL) of ethanol and water (9:1, mass ratio), and then the mixture was hydrolyzed for 3 h at room temperature. One gram of EG was added into a three-neck flask with the mixture and dispersed through ultrasonication (in water bath) for 30 min. After the reaction, the mixed solution was under backflow at 70°C for 3 h. The product was obtained by filtration and washing with water. The silane-treated EG was further dried in a vacuum oven at 80°C for 24 h. The obtained samples were named k-EG.

Hydroxylation of BT nanoparticles

Five grams of BT nanopowders was refluxed in 200 mL of an aqueous solution of H$_2$O$_2$ at 110°C for 6 h. Following reflux, suspended particles were filtered from the solution

and washed with deionized water at least seven times. Treated particles were dried in a vacuum oven at 80°C for 12 h. The generated powder was named as BT-OH.

Preparation of PVDF composites

The composites were prepared by solution cast method. At first, an amount of EG (0.5 wt%) was dispersed in DMAc by ultrasonic treatment for 30 min. At the same time, PVDF was dissolved in DMAc by magnetic stirring. The suspension of EG was then added into the PVDF/DMAc solution. Subsequently, the mixture was sonicated for 2 h and mechanically stirred at room temperature for 3 h. The composites were poured into uncovered glass dishes. The composites were then heated at 60°C for 12 h under a vacuum to evaporate the residual solution. The thickness of the composites was 200–300 μm. For comparison, PVDF, PVDF/k-EG (0.5 wt%), PVDF/k-EG (1 wt%), PVDF/BT-OH (0.5 wt%), PVDF/BT-OH (1 wt%), and PVDF/k-EG (0.5 wt%)/BT-OH (0.5 wt%) sheets were also prepared by the same method[29].

Characterization

Atomic force microscopic (Digital Instrument CSPM5500) measurements with the typical contact mode were performed to observe the morphology of different surface-functionalized EG. FTIR was acquired using a Bruker Tensor 27 system in the 4,000–500 cm^{-1} wave numbers to observe the change of chemical character of BT, BT-H, EG, and k-EG. All the samples were pressed into a pellet with potassium bromide before measurement. The surface morphologies of composites were characterized by SEM (FE-SEM, Hitachi-4800). EDS elemental mapping was collected using an energy dispersion of X-ray system equipped on FE-SEM S4800. The spectra were collected by cumulating 32 scans at a resolution of 2 cm^{-1}. The dielectric permittivity and dielectric loss of the composites were measured by the broadband dielectric spectroscopy (BDS) in the frequency 10^2–10^7 Hz, using an Alpha-N Frequency Response Analyzer, supplied by Novocontrol. A BDS-1200, parallel-plate capacitor with two gold-plated electrodes system, supplied also by Novocontrol, was used as dielectric test cell.

Results and discussion

Raman spectroscopy is a noninvasive technique, which is widely used to characterize the structural and electronic properties of the carbon-based materials such as carbon nanotubes, diamond, graphite, and diamond-like carbons. Structure change occurring from graphite to

EG is reflected in Figure 1. In Figure 1(a), as expected, graphite displays a prominent G peak as the only feature at 1,581 cm^{-1}, corresponding to the first-order scattering of the E2 g mode. In the Raman spectrum of graphene oxide, the G band is broadened and shifted to 1,594 cm^{-1}. In addition, the D band at 1,363 cm^{-1} becomes prominent, indicating the reduction in size of the in-plane sp^2 domains, possibly because of the extensive oxidation. The Raman spectrum of the EG also contains both G and D bands (at 1,584 and 1,352 cm^{-1}, respectively); however, with an increased I_D/I_G intensity ratio compared to that in graphene oxide. This change suggests a decrease in the average size of the sp^2 domains and can be explained if new graphitic domains were created that are smaller in size to the ones present in graphene oxide before reduction, but more numerous in number.

Exfoliated graphene and BT nanoparticles tend to form large aggregates because of their high surface energy and large surface area, which can lead to highly inhomogeneous films when simply blended in a
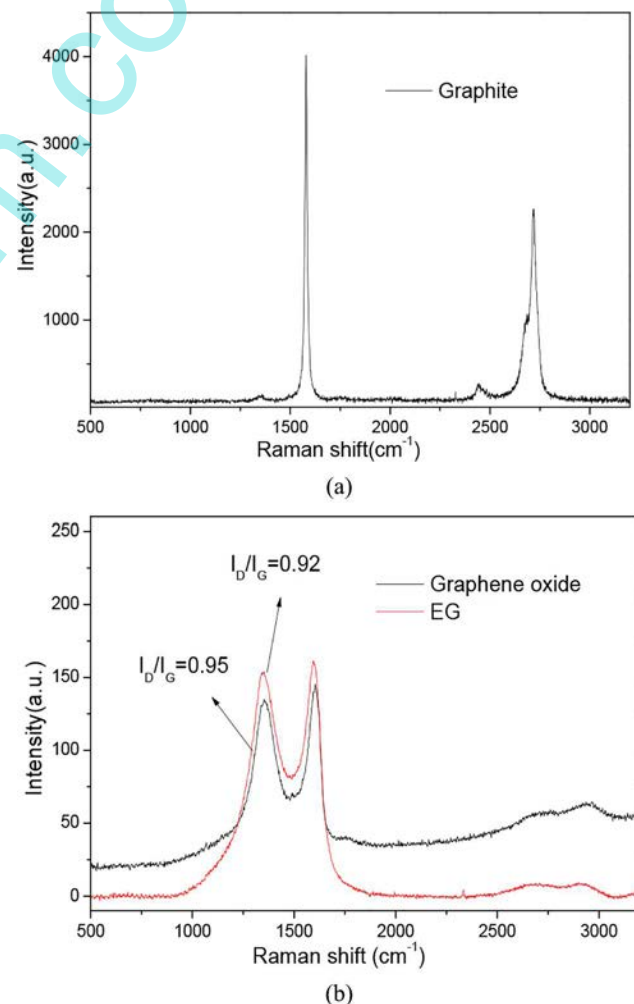

(a)

(b)

Figure 1. Raman spectra of (a) graphite and (b) graphene oxide and EG. *Note*: EG, exfoliated graphene.
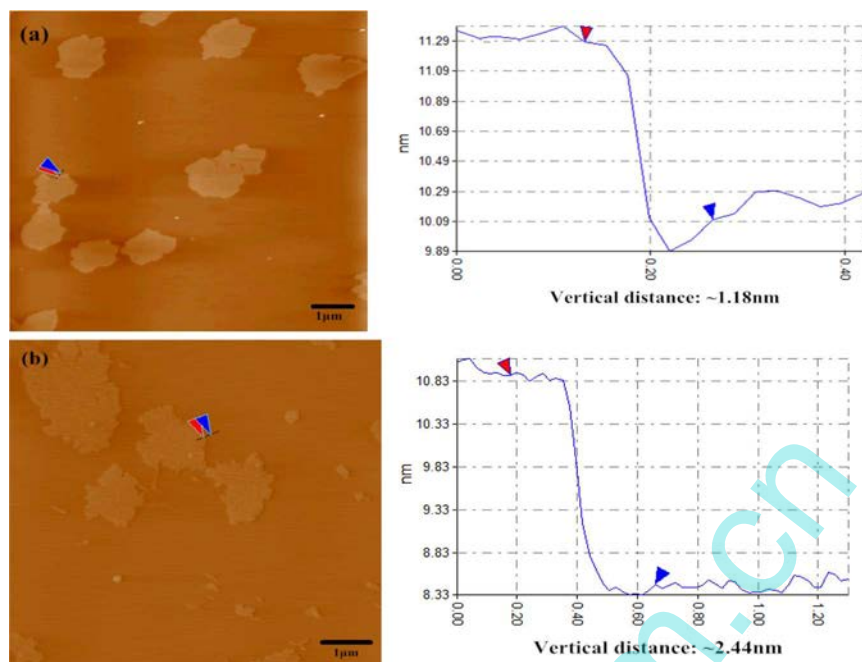
Figure 2. AFM images of (a) EG and (b) k-EG. *Note*: AFM, atomic force microscopic; EG, exfoliated graphene.

polymer matrix[47,48]. To mitigate this problem for incorporation of BT and EG into PVDF, they are treated by H_2O_2 and APTES, respectively. The mechanism for the functionalization was found by Lin et al. and Liu et al.[53,54] In this paper, the AFM image of the GOsuspension shown in Figure 2(a) offers a straightforward evidence for functionalization of graphene oxide (GO) sheets[52,55]. In Figure 2(a), the thickness of nanosheets we prepared is within 1.1–1.2 nm, as indicated in the contour curve. However, after silanization treatment, the thickness of the silane-treated EG sample is raised to 2.44 nm. The result reveals that the APTES chains were likely to attach onto the surface of EG. Furthermore, FTIR is used to testify the effect of the H_2O_2 treatment on the surface of the BT particles and the APTES treatment on the surface of the EG particles. Figure 3(a) shows the FTIR spectrum of EG. Pristine EG also showed –OH stretch at 1,383 cm^{-1}. For the silanized EG, two new bands at 2,918 and 2,854 cm^{-1} associated with the stretching of the methylene groups (–CH$_2$) from the APTES molecules appeared. Additionally, signals corresponding to C–N and Si–O stretches can be seen at 1,633 and 1,068 cm^{-1}, respectively. The appearance of new absorption peaks confirm that the APTES molecules are successfully attached onto the surface of EG[49]. As shown in Figure 3(b), the new band at 1,392 cm^{-1} is assigned to the vibration of –OH, which comes from the hydroxylation of BT-OH particles by the H_2O_2[53]. These results indicate that the surface treatment of the BT nanoparticles with H_2O_2 could endow the BT particles with –OH groups.
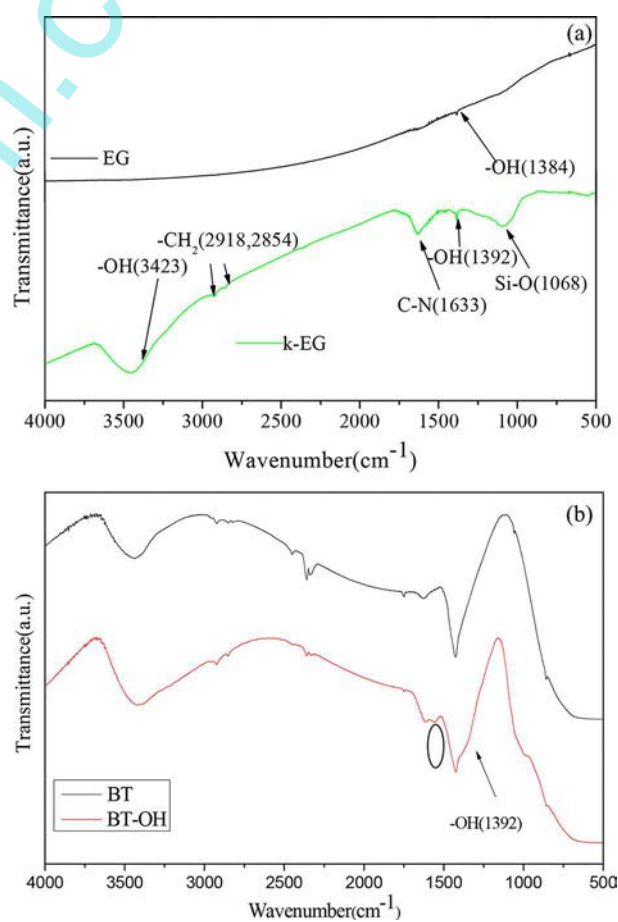

Figure 3. FTIR spectra for (a) EG and k-EG and (b) BT and BT-OH. *Note*: FTIR, Fourier transform infrared spectroscopy; EG, exfoliated graphene; BT, BaTiO$_3$.
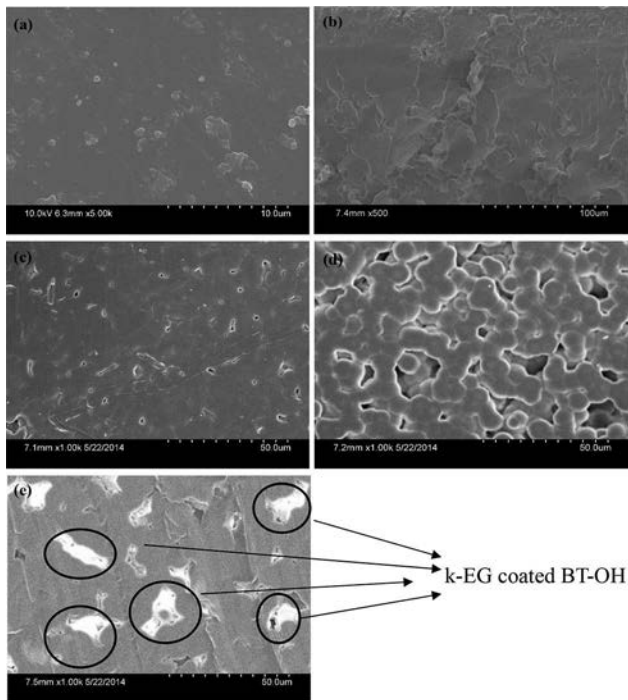
Figure 4. Free-fractured cross-sections of hybrid nanocomposite films of (a) PVDF, (b) 0.5 wt% EG/PVDF, (c) 0.5 wt% k-EG/PVDF, (d) 0.5 wt% BT-OH/PVDF, and (e) 0.5 wt% BT-OH/0.5 wt% k-EG/PVDF. *Note*: PVDF, poly(vinylidene fluoride); EG, exfoliated graphene; BT, BaTiO$_3$.

The microscopic homogeneity of the nanocomposite films was investigated by imaging the free-fractured cross sections of nanocomposite films using SEM. Compared with EG/PVDF, the k-EG formed uniform

and high-quality nanocomposite thin films in the PVDF host [Figure 4(b) and 4(c)]. For the cross section of BT-OH/PVDF, the agglomeration of BT-OH can be found obviously, which indicates a gloomy distribution of BT-OH nanoparticles in PVDF. However, this agglomeration seemed to be resolved by adding 0.5% k-EG. On one hand, different dimensions of BT-OH and k-EG are considered as the reason. On the other hand, it may be because of the fact that both of BT-OH and k-EG are electronegative so that aggregation of nanoparticles can be prohibited by each other.

Energy dispersive spectrometer elemental maps of Si (Figure 5a) and Ba [Figure 5(b) and 5(c)] clearly exhibit the dispersion of nanoparticles throughout the hybrid nanocomposite films. Figure 5(a) shows the well distribution of Si elements in nanocomposites, which implies the well dispersion of k-EG in PVDF films. In Figure 5(b), though BT is functionalized by H$_2$O$_2$, the agglomeration of Ba elements can be detected obviously, indicating the unfavorable dispersion of BT-OH in composites. However, this phenomenon could be resolved by mixing the BT-OH and k-EG together. As shown in Figure 5(c) and 5(d), the homogenous dispersion of Ba elements is realized in 0.5% BT-OH + 0.5% k-EG/PVDF composites, which is in good accordance with the results in Figure 4.

Dependence of dielectric constant of the PVDF nanocomposites as a function of frequency at room temperature is shown in Figures 6 and 7. As shown in Figure 6, the dielectric constant measured at lower frequency is
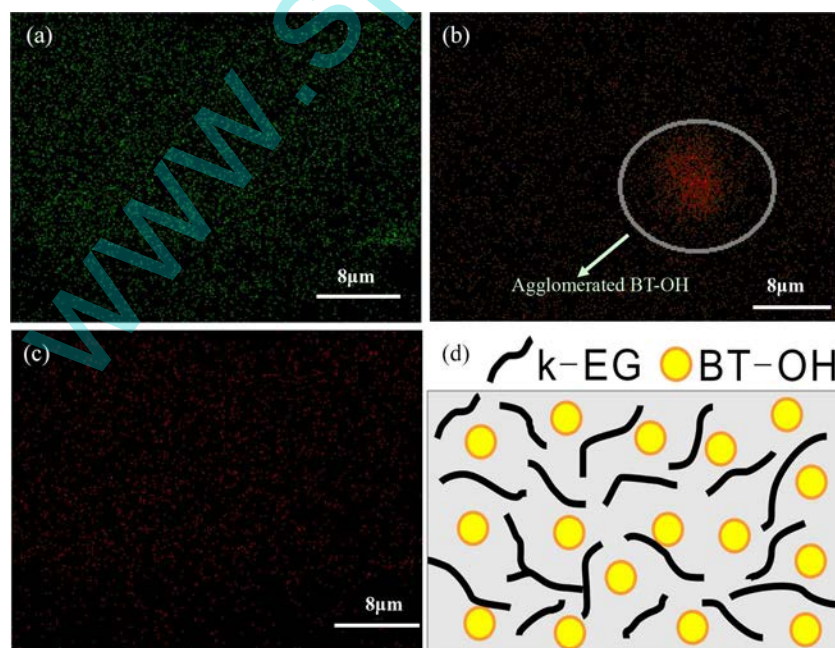

Figure 5. Distribution of Si elements in (a) 0.5% k-EG/PVDF and distribution of Ba element in (b) 0.5% BT-OH/PVDF, and (c) 0.5% BT-OH + 0.5% k-EG/PVDF. The schematic representation of the distribution of two nanoparticles in composites. *Note*: PVDF, poly(vinylidene fluoride); EG, exfoliated graphene; BT, BaTiO$_3$.
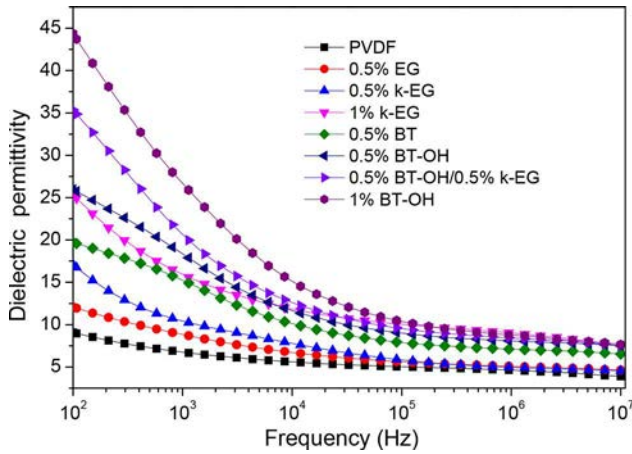
Figure 6. Dependence of effective dielectric permittivity on frequency at room temperature.

always greater than that at higher frequency. This frequency-dependent behavior is related to interfacial polarization, i.e., Maxwell–Wagner–Sillars polarization. For pure PVDF, the dielectric permittivity of pure PVDF gradually decreases from 9.8 to 4.0 ranged from 10^2 to 10^7 Hz. It can be clearly observed that the dielectric permittivity of the composites can be enhanced by blending with various nanoparticles, which may be induced by introducing high dielectric permittivity filler into the low dielectric PVDF host. In addition, with the increasing filler concentration, dielectric permittivity is increased obviously because of the higher polarization brought by the higher filler content[43].

Concerning about the effect of functionalizing nanoparticles, actually, the interface could significantly influence the dielectric performance of the composites[46]. When the functionalized particles are mixed with PVDF, chemical linkage for k-EG/PVDF, and hydrogen bonding for 0.5BT-OH/PVDF would be formed between the nanoparticles and PVDF, which both lead
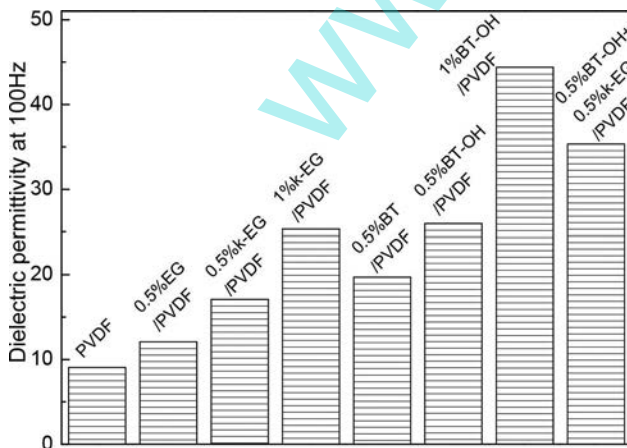
to fewer voids in the composites and bigger dielectric constant at 100 Hz than that of 0.5% EG/PVDF and 0.5% BT/PVDF.

Another interesting observation is that the dielectric permittivity of 0.5% k-EG + 0.5% BT-OH/PVDF is higher than that of 0.5% k-EG/PVDF and 0.5% BT-OH/PVDF. There might be two reasons. First, more filler content (1% actually for the former one and 0.5% for the latter composites) induces higher polarization for PVDF. Second, different dimensions for k-EG and BT-OH prohibit the agglomeration of nanoparticles, which makes a synergistic effect to improve the dielectric properties of composites. However, this synergistic effect is not so dramatic in improving the dielectric constant because of the fact that the value of the 0.5% k-EG + 0.5% BT-OH/PVDF is smaller than that of 1% BT-OH/PVDF.

Figure 8 shows the dielectric loss of the pure PVDF and PVDF-based nanocomposites as a function of frequency at room temperature. The loss tangent of nanocomposites is slightly higher than that of pure PVDF, which is due to the formation of interface between filler and base PVDF. Loss tangents for 0.5% EG/PVDF, 0.5% k-EG/PVDF, 1% k-EG/PVDF, 0.5% BT/PVDF, and 0.5% BT-OH/PVDF are similar to each other. The differences could be considered within the margin of error. However, the dielectric loss was remarkably increased after adding 1% BT-OH, which has the best effect in improving the dielectric constant in Figure 8. The percolation theory states that the variations of dielectric loss follow a power law as the filler content approaches the percolation threshold[50]. Furthermore, the poor BT-OH dispersion also causes difficulties in suppressing the dielectric loss of the composites[51].

Interestingly, the dielectric loss of the 0.5% k-EG + 0.5% BT-OH/PVDF composites is starkly lower than that of the PVDF nanocomposites with 1% BT-OH. Our interpretation of this behavior is based on the
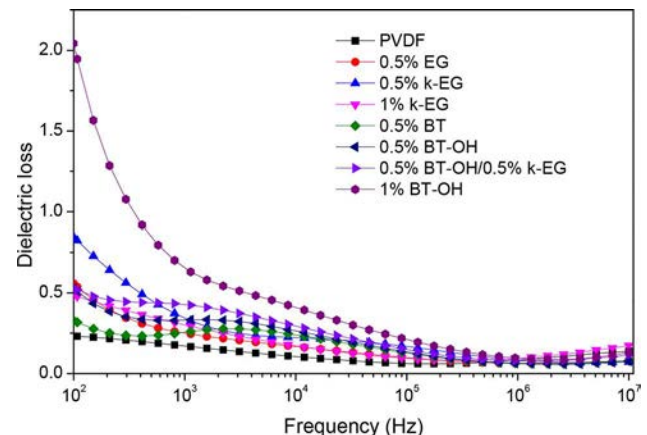

Figure 7. Dielectric permittivity of PVDF nanocomposites at 100 Hz. *Note*: PVDF, poly(vinylidene fluoride).

Figure 8. Dependence of dielectric loss on frequency at room temperature.

synergistic effect by blending the zero-dimensional BT-OH and two-dimensional k-EG together, which has been convinced by homogenous dispersion in Figure 5. Considering about the high dielectric constant and the low dielectric loss, the synergistic 0.5% k-EG + 0.5% BT-OH/PVDF shows an attractive prospect in application.

Conclusion

We report a PVDF composite reinforced by hybrid nanoparticles of k-EG (0.5 wt%) +BT-OH (0.5 wt%) with an efficient solution cast method. For comparison, the composites with EG (0.5 wt%), k-EG (0.5 wt%), k-EG (1 wt%), BT (0.5 wt%), BT-OH (0.5 wt%), and BT-OH (1 wt%) are also prepared and their dielectric properties are characterized. BT and EG are primarily functionalized before using. AFM and FTIR results prove that APTES chains and –OH groups are successfully attached onto the surface of k-EG and BT-OH, respectively. Second, SEM and EDS characterizations show that the distribution of BT-OH in PVDF host is not desirable. However, this agglomeration of BT-OH seemed to be resolved by adding 0.5% k-EG. Different dimensions and the same electronegative properties of BT-OH and k-EG are considered to be the reasons for dispersing fillers homogenously. Finally, dielectric performance tests reveal that functionalization of nanoparticles and increasing the filler contents could both improve the dielectric permittivity. Specially, the composite with 0.5% k-EG + 0.5% BT-OH shows great prospects in application for its high dielectric constant and low loss tangent. Synergistic effect by blending the zero-dimensional BT-OH and two-dimensional k-EG together is thought to be the main reason for this phenomenon.

Funding

References

[1] Kelarakis, A.; Hayrapetyan, S.; Ansari, S.; Fang, J.; Estevez, L.; Giannelis, E.P. Clay nanocomposites based on poly(vinylidene fluoride-co-hexafluoropropylene): Structure and properties. Polymer **2010**, *51* (2), 469–474.

[2] Tong, W.; Zhang, Y.; Yu, L.; Luan, X.; An, Q.; Zhang, Q.; Lv, F.; Chu, P.K.; Shen, B.; Zhang, Z. Novel method for the fabrication of flexible film with oriented arrays of graphene in poly(vinylidene fluoride-co-hexafluoropropylene) with low dielectric loss. J. Phys. Chem. C **2014**, *118* (20), 10567–10573.

[3] Yu, S.; Zheng, W.; Yu, W.; Zhang, Y.; Jiang, Q.; Zhao, Z. Formation mechanism of beta-phase in PVDF/CNT composite prepared by the sonication method. Macromolecules **2009**, *42* (22), 8870–8874.

[4] Fan, P.; Wang, L.; Yang, J.; Chen, F.; Zhong, M. Graphene/poly(vinylidene fluoride) composites with high dielectric constant and low percolation threshold. Nanotechnology **2012**, *23* (36).

[5] Su, Y.L.; Sun, C.; Zhang, W.Q.; Huang, H. Fabrication and dielectric properties of $Na_{0.5}Bi_{0.5}Cu_3Ti_4O_{12}$/poly (vinylidene fluoride) composites. J. Mater. Sci. **2013**, *48* (23), 8147–8152.

[6] Mishra, P.; Kumar, P. Dielectric properties of 0.25(BZT–BCT)–0.75 $(1 - x)$PVDF–xCCTO ($x = 0.02$, 0.04, 0.06, 0.08 and 0.1) composites for embedded capacitor applications. Compos. Sci. Technol. **2013**, 8826–8832.

[7] Zha, J.W.; Dang, Z.M.; Yang, T.; Zhou, T.; Song, H.T.; Li, S.T. Advanced dielectric properties of $BaTiO_3$/polyvinylidene-fluoride nanocomposites with sandwich multi-layer structure. IEEE Trans. Dielectr. Electr. Insul. **2012**, *19* (4), 1312–1317.

[8] Zhang, L.; Shan, X.; Wu, P.; Cheng, Z.Y. Dielectric characteristics of $CaCu_3Ti_4O_{12}$/P(VDF-TrFE) nanocomposites. Appl. Phys. A **2012**, *107* (3), 597–602.

[9] Xia, W.; Xu, Z.; Wen, F.; Zhang, Z. Electrical energy density and dielectric properties of poly(vinylidene fluoride-chlorotrifluoroethylene)/$BaSrTiO_3$ nanocomposites. Ceram. Int. **2012**, *38* (2), 1071–1075.

[10] Shang, J.; Zhang, Y.; Yu, L.; Shen, B.; Lv, F.; Chu, P.K. Fabrication and dielectric properties of oriented polyvinylidene fluoride nanocomposites incorporated with graphene nanosheets. Mater. Chem. Phys. **2012**, *134* (2–3), 867–874.

[11] Bhadra, D.; Masud, M.G.; Sarkar, S.; Sannigrahi, J.; De, S.K.; Chaudhuri, B.K. Synthesis of PVDF/$BiFeO_3$ nanocomposite and observation of enhanced electrical conductivity and low-loss dielectric permittivity at percolation threshold. J. Polym. Sci. Part B **2012**, *50* (8), 572–579.

[12] Li, Y.; Tjong, S.C. Structure and electrical characteristics of poly(vinylidene fluoride) filled with beta silicon carbide nanoparticles. J. Nanosci. Nanotechnol. **2011**, *11* (6), 5148–5153.

[13] Thomas, P.; Satapathy, S.; Dwarakanath, K.; Varma, K.B.R. Dielectric properties of poly(vinylidene fluoride)/$CaCu_3Ti_4O_{12}$ nanocrystal composite thick films. Express Polym. Lett. **2010**, *4* (10), 632–643.

[14] Arbatti, M.; Shan, X.B.; Cheng, Z.Y. Ceramic-polymer composites with high dielectric constant. Adv. Mater. **2007**, *19* (10), 1369–1372.

[15] Feng, Y.; Li, W.L.; Hou, Y.F.; Yu, Y.; Cao, W.P.; Zhang, T.D.; Fei, W.D. Enhanced dielectric properties of PVDF-HFP/$BaTiO_3$-nanowire composites induced by interfacial polarization and wire-shape. J. Mater. Chem. C **2015**, *3* (6), 1250–1260.

[16] Deepa, K.S.; Shaiju, P.; Sebastian, M.T.; Gowd, E.B.; James, J. Poly(vinylidene fluoride)-$La_{0.5}Sr_{0.5}CoO_3$-delta composites: The influence of LSCO particle size on the

structure and dielectric properties. Phys. Chem. Chem. Phys. **2014**, *16* (32), 17008–17017.

[17] Wang, Y.P.; Peng, Z.J. Performance of Ba0.95Ca0.05Zr0.15Ti0.85O3/PVDF composite flexible films. J. Ceram. Soc. Japan **2014**, *122* (1428), 719–724.

[18] Srivastava, A.; Maiti, P.; Kumar, D.; Parkash, O. Mechanical and dielectric properties of $CaCu_3Ti_4O_{12}$ and La doped $CaCu_3Ti_4O_{12}$ poly(vinylidene fluoride) composites. Compos. Sci. Technol. **2014**, 9383–9389.

[19] Xie, L.Y.; Huang, X.Y.; Yang, K.; Li, S.T.; Jiang, P.K. "Grafting to" route to PVDF-HFP-GMA/$BaTiO_3$ nanocomposites with high dielectric constant and high thermal conductivity for energy storage and thermal management applications. J. Mater. Chem. A **2014**, *2* (15), 5244–5251.

[20] Chiolerio, A.; Lombardi, M.; Guerriero, A.; Canavese, G.; Stassi, S.; Gazia, R.; Cauda, V.; Manfredi, D.; Chiodoni, A.; Verna, A.; Cocuzza, M.; Montanaro, L.; Pirri, C.F. Effect of the fabrication method on the functional properties of $BaTiO_3$: PVDF nanocomposites. J. Mater. Sci. **2013**, *48* (20), 6943–6951.

[21] Kuang, X.; Lin, S.; Zhu, H. Synthesis and characterization of poly(vinylidene-trifluoroethylene)/Ni–TiO_2. Phys. Status Solidi A **2013**, *210* (3), 570–573.

[22] Lin, M.F.; Lee, P.S. Formation of PVDF-g-HEMA/$BaTiO_3$ nanocomposites via in situ nanoparticle synthesis for high performance capacitor applications. J. Mater. Chem. A **2013**, *1* (46), 14455–14459.

[23] Lin, S.; Kuang, X.W.; Wang, F.H.; Zhu, H. Effect of TiO_2 crystalline composition on the dielectric properties of TiO_2/P(VDF-TrFE) composites. Phys. Status Solidi **2012**, *6* (8), 352–354.

[24] Liu, S.H.; Xue, S.X.; Zhang, W.Q.; Zhai, J.W.; Chen, G.H. Significantly enhanced dielectric property in PVDF nanocomposites flexible films through a small loading of surface-hydroxylated $Ba_{0.6}Sr_{0.4}TiO_3$ nanotubes. J. Mater. Chem. A **2014**, *2* (42), 18040–18046.

[25] Ning, N.Y.; Bai, X.; Yang, D.; Zhang, L.Q.; Lu, Y.L.; Nishi, T.; Tian, M. Dramatically improved dielectric properties of polymer composites by controlling the alignment of carbon nanotubes in matrix. RSC Adv. **2014**, *4* (9), 4543–4551.

[26] Lai, M.B.; Yu, S.H.; Sun, R.; Zeng, X.L.; Luo, S.B.; Wong, C.P. Effects and mechanism of graft modification on the dielectric performance of polymer-matrix composites. Compos. Sci. Technol. **2013**, *89*, 127–133.

[27] Mandal, B.P.; Vasundhara, K.; Abdelhamid, E.; Lawes, G.; Salunke, H.G.; Tyagi, A.K. Improvement of magneto-dielectric coupling by surface functionalization of nickel nanoparticles in Ni and polyvinylidene fluoride nanohybrids. J. Phys. Chem. C **2014**, *118* (36), 20819–20825.

[28] Dalle Vacche, S.; Oliveira, F.; Leterrier, Y.; Michaud, V.; Damjanovic, D.; Manson, J.A.E. Effect of silane coupling agent on the morphology, structure, and properties of poly(vinylidene fluoride-trifluoroethylene)/$BaTiO_3$ composites. J. Mater. Sci. **2014**, *49* (13), 4552–4564.

[29] Wang, S.; Liu, L.; Zeng, Y.; Zhou, B.; Teng, K.; Ma, M.; Chen, L.; Xu, Z. Improving dielectric properties of poly (vinylidene fluoride) composites: Effects of surface functionalization of exfoliated graphene. J. Adhes. Sci. Technol. **2015**, *29* (7), 678–690.

[30] Wu, Y.; Lin, X.Y.; Shen, X.; Sun, X.Y.; Liu, X.; Wang, Z.Y.; Kim, J.K. Exceptional dielectric properties of chlorine-doped graphene oxide/poly (vinylidene fluoride) nanocomposites. Carbon **2015**, *89*, 102–112.

[31] Yang, C.; Song, H.S.; Liu, D.B. Effect of coupling agents on the dielectric properties of $CaCu_3Ti_4O_{12}$/PVDF composites. Compos. Part B **2013**, *50*, 180–186.

[32] Shang, J.; Zhang, Y.; Yu, L.; Luan, X.; Shen, B.; Zhang, Z.; Lv, F.; Chu, P.K. Fabrication and enhanced dielectric properties of graphene-polyvinylidene fluoride functional hybrid films with a polyaniline interlayer. J. Mater. Chem. A **2013**, *1* (3), 884–890.

[33] Liu, S.; Xiao, S.; Xiu, S.; Shen, B.; Zhai, J.; An, Z. Poly (vinylidene fluoride) nanocomposite capacitors with a significantly enhanced dielectric constant and energy density by filling with surface-fluorinated $Ba_{0.6}Sr_{0.4}TiO_3$ nanofibers. RSC Adv. **2015**, *5* (51), 40692–40699.

[34] Chen, G.X.; Zhang, S.C.; Zhou, Z.; Li, Q.F. Dielectric properties of poly(vinylidene fluoride) composites based on bucky gels of carbon nanotubes with ionic liquids. Polym. Compos. **2015**, *36* (1), 94–101.

[35] Zhang, X.H.; Ma, Y.H.; Zhao, C.W.; Yang, W.T. High dielectric performance composites with a hybrid $BaTiO_3$/graphene as filler and poly(vinylidene fluoride) as matrix. ECS J. Solid State Sci. Technol. **2015**, *4* (5), N47–N54.

[36] Yuan, J.K.; Li, W.L.; Yao, S.H.; Lin, Y.Q.; Sylvestre, A.; Bai, J.B. High dielectric permittivity and low percolation threshold in polymer composites based on SiC-carbon nanotubes micro/nano hybrid. Appl. Phys. Lett. **2011**, *98* (3).

[37] Chanmal, C.V.; Jog, J.P. Dielectric relaxations in PVDF/$BaTiO_3$ nanocomposites. Express Polym. Lett. **2008**, *2* (4), 294–301.

[38] Wu, C.; Huang, X.Y.; Xie, L.Y.; Yu, J.H.; Jiang, P.K. Morphology-controllable graphene-TiO_2 nanorod hybrid nanostructures for polymer composites with high dielectric performance. J. Mater. Chem. **2011**, *21* (44), 17729–17736.

[39] Li, Y.; Huang, X.; Hu, Z.; Jiang, P.; Li, S.; Tanaka, T. Large dielectric constant and high thermal conductivity in poly(vinylidene fluoride)/barium titanate/silicon carbide three-phase nanocomposites. ACS Appl. Mater. Interfaces **2011**, *3* (11), 4396–4403.

[40] Yang, L.; Qiu, J.; Ji, H.; Zhu, K.; Wang, J. Enhanced dielectric and ferroelectric properties induced by TiO_2@MWCNTs nanoparticles in flexible poly(vinylidene fluoride) composites. Compos. Part A **2014**, *65*, 125–134.

[41] Khadheer, P.S.K.; Deshmukh, K.; Ahamed, M.B.; Chidambaram, K.; Mohanapriya, M.K.; Arunal, N.R.N. Investigation of microstructure, morphology, mechanical, and dielectric properties of PVA/PbO nanocomposites. Adv. Polym. Technol. **2015**.

[42] Deshmukh, K.; Ahamed, M.B.; Deshmukhb, R.R.; Bhagatc, P.R.; Khadeer, P.S.K.; Bhagate, A.; Shirbhatee, R.; Telaree, F.; Lakhanif, C. Influence of K_2CrO_4 doping on the structural, optical and dielectric properties of polyvinyl alcohol/K_2CrO_4 composite films. Polym. Plast. Technol. Eng. **2015**. doi:10.1080/03602559.2015.1055499.

[43] Deshmukh, K.; Ahamed, M.B.; Khadeer, P.S.K.; Deshmukh, R.R.; Bhagat, P.R. Highly dispersible graphene oxide reinforced polypyrrole/polyvinyl alcohol blend

nanocomposites with high dielectric constant and low dielectric loss. RSC Adv. **2015**, *5*, 61933–61945.

[44] Deshmukh, K.; Ahamed, M.B.; Deshmukh, R.R.; Pasha, S.K.; Sadasivuni, K.K.; Ponnamma, D.; Chidambaram, K. Synergistic effect of vanadium pentoxide and graphene oxide in polyvinyl alcohol for energy storage application. Eur. Polym. J. **2016**, *76*, 14–27.

[45] Luo, S.B.; Yu, S.H.; Sun, R.; Wong, C.P. Nano Ag-deposited BaTiO₃ hybrid particles as fillers for polymeric dielectric composites: Toward high dielectric constant and suppressed loss. ACS Appl. Mater. Interfaces **2014**, *6* (1), 176–182.

[46] Liu, Z.D.; Feng, Y.; Li, W.L. High dielectric constant and low loss of polymeric dielectric composites filled by carbon nanotubes adhering BaTiO₃ hybrid particles. RSC Adv. **2015**, *5* (37), 29017–29021.

[47] Kim, P.; Doss, N.M.; Tillotson, J.P.; Hotchkiss, P.J.; Pan, M.-J.; Marder, S.R.; Li, J.; Calame, J.P.; Perry, J.W. High energy density nanocomposites based on surface-modified BaTiO₃ and a ferroelectric Polymer. Acs Nano. **2009**, *3* (9), 2581–2592.

[48] Khodaparast, P.; Ounaies, Z. Influence of dispersion states on the performance of polymer-based nanocomposites. Smart Mater. Struct. **2014**, *23* (10).

[49] Chen, L.; Jin, H.; Xu, Z.; Shan, M.; Tian, X.; Yang, C.; Wang, Z.; Cheng, B. A design of gradient interphase reinforced by silanized graphene oxide and its effect on carbon fiber/epoxy interface. Mater. Chem. Phys. **2014**, *145* (1–2), 186–196.

[50] Zhou, T.; Zha, J.-W.; Cui, R.-Y.; Fan, B.-H.; Yuan, J.-K.; Dang, Z.-M. Improving dielectric properties of BaTiO₃/ferroelectric polymer composites by employing surface hydroxylated BaTiO₃ nanoparticles. ACS Appl. Mater. Interfaces **2011**, *3* (7), 2184–2188.

[51] Xu, Z.W.; Yue, M.Y.; Chen, L.; Zhou, B.M.; Shan, M.J.; Niu, J.R.; Li, B.D.; Qian, X.M. A facile preparation of edge etching, porous and highly reactive graphene nanosheets via ozone treatment at a moderate temperature. Chem. Eng. J. **2014**, *240*, 187–194.

[52] Wang, S.J.; Geng, Y.; Zheng, Q.B.; Kim, J.K. Fabrication of highly conducting and transparent graphene films. Carbon **2010**, *48* (6), 1815–1823.

[53] Almadhoun, M.N.; Bhansali, U.S.; Alshareef, H.N. Nanocomposites of ferroelectric polymers with surface-hydroxylated BaTiO₃ nanoparticles for energy storage applications. J. Mater. Chem. **2012**, *22* (22), 11196–11200.

[54] Wang, D.; Bao, Y.; Zha, J.-W.; Zhao, J.; Dang, Z.-M.; Hu, G.-H. Improved dielectric properties of nanocomposites based on poly(vinylidene fluoride) and poly(vinyl alcohol)-functionalized graphene. ACS Appl. Mater. Interfaces **2012**, *4* (11), 6273–6279.

[55] Yang, K.; Huang, X.Y.; Fang, L.J.; He, J.L.; Jiang, P.K. Fluoro-polymer functionalized graphene for flexible ferroelectric polymer-based high-k nanocomposites with suppressed dielectric loss and low percolation threshold. Nanoscale **2014**, *6* (24), 14740–14753.